iScience

CellPress
OPEN ACCESS

Article

Synthesizing nuclear power plant fouling with fractal characteristics enables an in-depth study of concerned nuclear safety issues

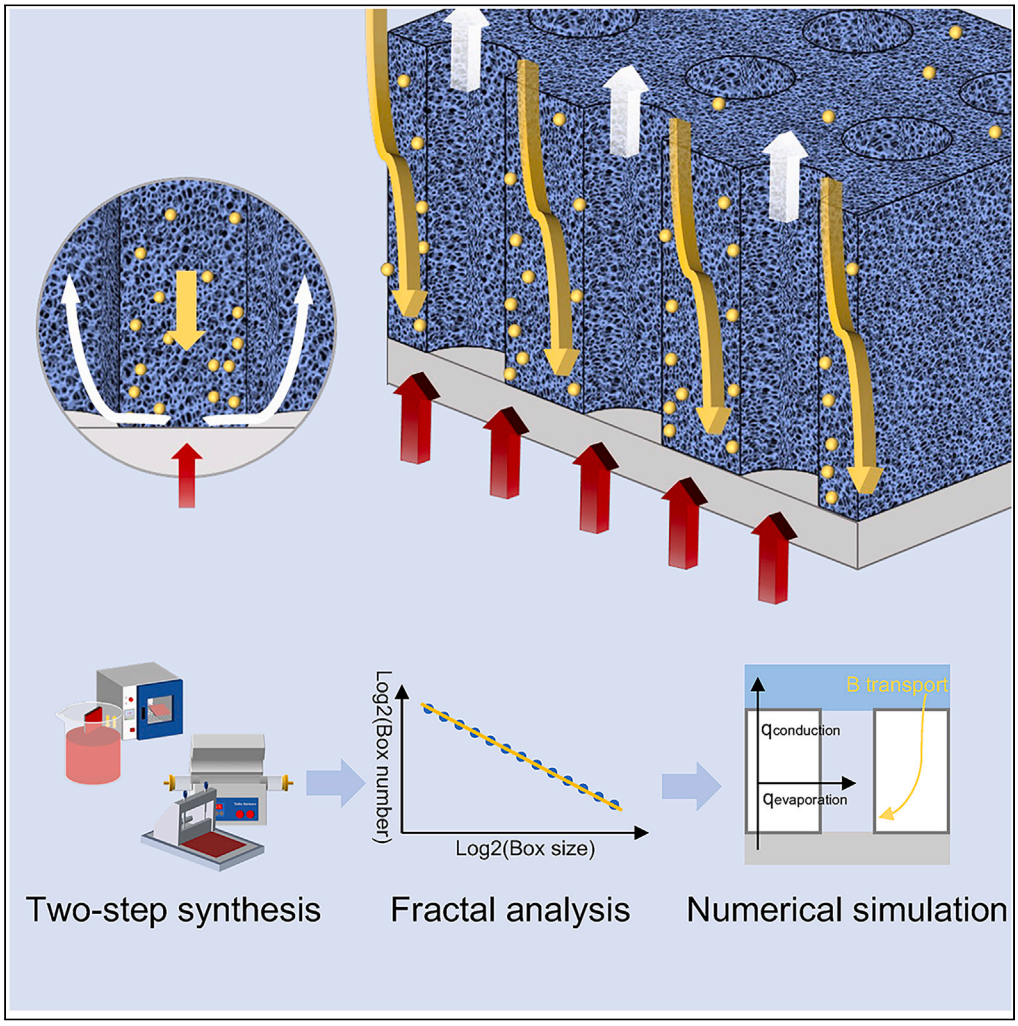

Yan Liu, Xiaojing Liu, Hui He, Tengfei Zhang, Xiang Chai

xiaojingliu@sjtu.edu.cn

Highlights

Fast synthesis of fouling deposit with structural self-similarity by two-step method

Unified porosity-fractal dimension relation for micro-structure of fouling deposit

High-precision prediction of wick boiling and boron hideout via fractal dimension

Liu et al., iScience *27*, 108789
February 16, 2024
https://doi.org/10.1016/j.isci.2024.108789

iScience

CellPress
OPEN ACCESS

Article

Synthesizing nuclear power plant fouling with fractal characteristics enables an in-depth study of concerned nuclear safety issues

Yan Liu,[1] Xiaojing Liu,[1,2,*] Hui He,[1] Tengfei Zhang,[1] and Xiang Chai[1]

SUMMARY

Fouling deposit on nuclear fuel cladding causes wick boiling and boron hideout, resulting in localized corrosion and power shift with great potential security and economic risks. Herein, a cost-effective time-saving adjustable reproduction method combining sol-gel with ceramic sintering is presented to enable wide coverage of fouling's morphologies and microstructures. Based on fractal analysis, structurally self-similar fouling deposits from different reactors conform to proposed porosity-fractal dimension law under 3% relative error. Wick boiling and boron hideout numerical simulation based on fractal dimension is implemented to treat different morphologies and structures in a unified way. Cladding surface underneath fouling deposit has a maximum 9.243 K temperature increasement due to thermal resistance, and H_3BO_3 is concentrated 11.274 times by mean of wick boiling, causing $Li_2B_4O_7$ precipitation under extreme conditions with low porosity and high heat flux. The insights in this study provide a precise approach for quantitative evaluation of localized corrosion and power shift.

INTRODUCTION

The fouling deposit named corrosion-related unidentified deposit (CRUD) occurs in pressurized water reactors due to the deposition of corrosion products in the primary loop coolant on the fuel rod cladding surfaces at the upper part of reactor cores. As negative by-products, despite wick boiling at the end of the fouling deposit's micro-channels can enhance heat transfer, as the deposit grow to a certain thickness CRUD usually impedes heat transfer and elevates cladding temperature, leading to cladding corrosion (CRUD-induced localized corrosion, CILC). Also, the wick boiling makes aqueous solutes become supersaturated and eventually precipitate. Among the concentrated solutes, boric acid and any other boron-containing species are strong neutron absorbers, and the boron hideout within CRUD results in a depression in the local neutron flux and local power output at the upper half of the core. The depression causes an abnormal power distribution in the core, known as CRUD-induced power shift (CIPS), which has been proven to be the most significant fuel performance concern associated with CRUD,[1] as depicted in Figure 1A. Several nuclear power plants worldwide have experienced CIPS and the resulting significant operational and economic consequences. The most famous CIPS is that Callaway plant had to downrate its power to approximately 75% for the final third of Cycle 9 to increase the safety margin and recover the shutdown margin, resulting in an estimated economic penalty of $20 M. CIPS also has an impact on the next cycle, for example, Callaway Cycle 10 experienced CIPS at the beginning of the cycle, which increased the difficulty of the reactor start-up operation. Some utilities purchased additional fuel assemblies to reduce the susceptibility of CIPS, costing anywhere from $0.5 M to $2 M per cycle.[1] Since CRUD will bring potential threats and uncertainties to the safe and economic operation of pressurized water reactor (PWR), international scholars have studied the fuel performance concern caused by corrosion products in the reactor core and its incentives.[2–6] Given the huge economic losses caused by CIPS, CASL (Consortium for Advanced Simulation of Light Water Reactors) has identified the fuel performance problem caused by CRUD as a key technical challenge to limit the future industrial upgrading of nuclear energy.[7] Accurate simulation and prediction of CIPS can help prevent accidental power plant downrating and unplanned outages to avoid economic losses.

However, due to the harsh environment of the reactor, it is still challenging to observe CRUD directly or run experiments in reactor core. Although the CRUD samples obtained from reactors allow CRUD morphology measurement, these samples are still impossible to be used to carry out a heat transfer and boron hideout experimental study on the mechanism. On the one hand, the cooling and depressurization of the reactor shutdown and the subsequent cleaning process make the boron species trapped in the CRUD return to the bulk coolant (mainstream area) again.[8] Boric acid or boron lithium compounds to date have not been found directly in the CRUD samples,[1] which cannot directly obtain the distribution law of boron. On the other hand, neutrons activate Fe, Ni, and Cr in CRUD (e.g., $^{58}Ni(n,p)^{58}Co$), resulting in high radioactivity of CRUD samples,[1] which increases the research cost, uncertainty, and security risks. Therefore, it is necessary to reproduce CRUD with

[1]School of Mechanical Engineering, Shanghai Jiao Tong University, Shanghai 200240, China
[2]Lead contact
*Correspondence: xiaojingliu@sjtu.edu.cn
https://doi.org/10.1016/j.isci.2024.108789

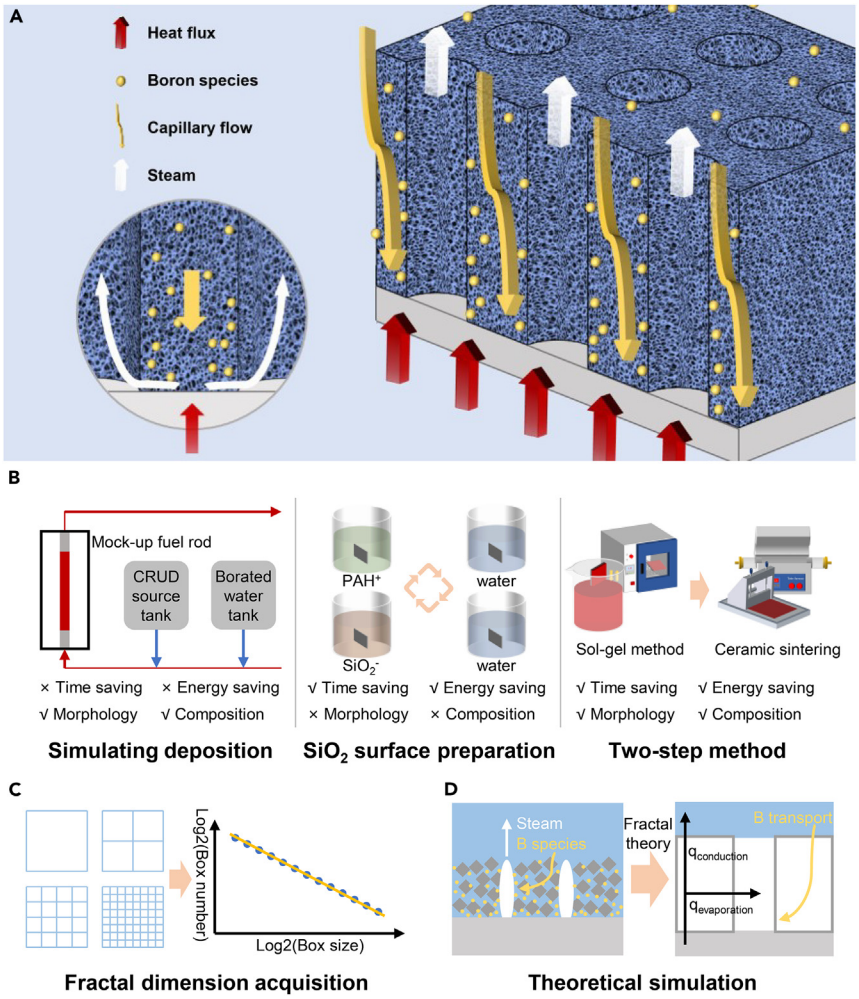

Figure 1. Schematic diagram of the methodology used to synthesize fouling deposit quickly and simulate wick boiling and boron hideout within fouling deposit theoretically

(A) Wick boiling and boron hideout phenomena in fouling deposit.

(B) Comparison of synthesis methods and the advantages of two-step method.

(C) Acquisition of fractal dimension of fouling deposit via box-counting method.

(D) Simulation of wick boiling and boron hideout of a chimney structure unit.

morphology and micro-structure similar to real one by compromise methods. In general, there are two main research ideas: deposition preparation by simulating reactor thermal and water chemical conditions[2,3,6] and preparation via thin film technique.[9] Relatively speaking, the former method is far more time-consuming and costly than the latter, since deposition preparation needs to simulate the harsh operating conditions of the reactor. Thin film technique can form a technical route for the rapid preparation of CRUD samples and save the cost and time of reproduction process, which seems to be a promising method for exploratory experiments on wick boiling and boron hideout. However, only a few studies on the preparation of thin film technique have been carried out, and they tend to use silica instead of iron-nickel oxide as a replica material to obtain depositions with approximate total thermal resistance.[9] The comparison of these synthesis methods and their technology indices is shown in Figure 1B.

At present, the CRUD morphologies and components of different nuclear power plants reported publicly are quite different. It is generally believed that the thermal hydraulics, water chemistry, neutron environment, and even fuel rod orientation influence the morphologies and components of CRUD depositions.[1] But there are still some common points that CRUD is a naturally occurring hydrophilic porous medium composed of iron-nickel oxides, with its thickness, porosity, and roughness values varying greatly. In general, the thickness is between 10 and 100 μm, the average pore size is between 0.1 and 1 μm, the porosity ranges from 40% to 70%, and the roughness ranges from 0.5 to 3.0 μm[1]. Based on the morphology analysis and theoretical derivation, some codes have theoretically predicted the heat and mass transfer within the CRUD depositions, including Boron-induced Offset Anomaly[10,11] developed by Electric Power Research Institute (EPRI) and MPO advanced model for boron analysis[12] developed by CASL. Of practical interest from these codes, the heat is conducted away from the cladding of fuel

rod and lost gradually via the wick boiling at the chimney surface, while sufficient coolant with solutes including boron acid and lithium ion enters the CRUD to replace the evaporative loss under the action of capillary force to maintain the liquid phase equilibrium and chemical equilibrium in the CRUD.[10–13] Additionally, these codes more or less consider the chemical reactions between solutes and their interaction with neutrons in the coolant, and also consider the effect of solute solubility on saturation temperature, which has a great influence on the prediction of subcooled boiling. However, because there is no unified method to deal with the different complex structures of CRUD in different reactors, it is difficult to obtain accurate internal physical phenomenon parameters for different cases, limiting the wide application ability of these codes.

In recent years, with the continuous acquisition of experimental data related to heat transfer and water chemistry, obtaining more accurate physical parameters in the porous CRUD has become a way to improve the accuracy of the code prediction.[10,14] To study the wick boiling heat transfer and boron hideout within the CRUD depositions, overall properties of CRUD such as density, average pore sizes, average porosity, and average heat conductivity are insufficient. Based on statistical self-similarity, which means the local structure is similar to the whole, fractals or fractalline shapes have been proven to be able to better describe complex materials in nature and engineering,[15] including ocean coastlines[16] and sintered powder metallurgy components.[17] Also, the fouling deposits similar to CRUD have shown self-similarity of fractallines to a certain extent, such as salt crystallization deposition,[18] bio-membrane sludge,[19] and $CaCO_3$ deposition during boiling in heat exchangers.[20] Despite CRUD depositions having highly complex porous structures, it can be considered that the introduction of the fractal analysis method for these similar fouling deposits can help analyze CRUD to characterize materials properties, such as permeability, heat transfer, and diffusivity quantitatively. For porous materials with fractal characteristics, fractal dimension is an important parameter to quantitatively describe the degree of self-similarity, which is often related to porosity. However, to date, the relationship between CRUD porosity and fractal dimension is still lacking. The use of fractal dimension related to porosity can give a more comprehensive introduction to the pore distribution and pore sizes and help calculate thermal conductivity and fluid permeability property, which has a significant impact on the heat and mass transfer characteristics within the CRUD depositions.

To address these challenges, a fast two-step method to synthesize CRUD based on sol-gel method and ceramic sintering method is proposed (Figure 1B). The analysis of the CRUD synthesis process and real CRUD formation shows the similarities and differences in crystal formation, growth, and porous formation, which proves the feasibility of two-step synthesis. Through scanning electron microscopy and image processing (Figure 1C), despite different morphologies, the micro-structures of CRUD produced by different methods can be regarded as self-similarity materials and are unified in fractal dimension. The consistency of the relationship between porosity and fractal dimension also suggests the representativeness of synthetic CRUD for the samples in PWR. Based on the proposed unified relationship between porosity and fractal dimension, the simulation of wick boiling and boron hideout is carried out (Figure 1D), and the effects of CRUD porosity, heat flux, and bulk coolant boron concentration are investigated and discussed in detail.

RESULTS AND DISCUSSION

Synthetic CRUD characterization

Figure 2 shows the characterization of three synthetic CRUD samples obtained by using the same sol-gel parameters to prepare the inner layer and sintering nanoparticles (95 wt. % nickel ferrite and 5 wt. % iron oxide) with different particle sizes to prepare the outer layers. As shown in Figure 2A, under the same conditions of other parameters, the outer layer pore sizes can be effectively increased by increasing the nanopowder particle size. From left to right, the average pore sizes on the outer layer surfaces are about 100, 500, and 800 nm, respectively, with the used nanopowders particle sizes of about 50, 250, and 500 nm, which are agglomerated and increased during the sintering process. In the rightmost figure, a small amount of pores reached about 1 μm. In Figure 2B, both nano-sized pores and a small amount of micron-sized long nano-sized wide narrow pores appear on synthetic CRUD inner surface, with average pore size of about 250 nm, which is within the parameter range of the real CRUD.[21] The porosity of the outer layer is related to the component of the paste. When the nanopowders increase from 30.00 wt. % to 41.67 wt. %, the porosity decreases approximately from 60.40% to 39.48% (Note S4). The thickness is mainly related to the number of wet film pulling and the thickness of the paste coating. The inner layer can reach a maximum of about 20 μm after increasing the number of wet film pulling with some cracks in local areas, and the outer layer thickness can reach 100 μm, which covers the thickness range of the real CRUD. There are large pores named "chimney" structures on the surface of the outer layer with a diameter of several microns, which is considered to be one of the channels for gas escape during sintering, but this structure is not evenly distributed. Its position and inclination (see Figure 2C) are mainly related to the direction of the airflow during the sintering process, which is also similar to the real CRUD.[21] The porosity and thickness of CRUD are measured after gray threshold processing. The chimney diameter of synthetic CRUD is between 2 and 9 μm, mainly concentrated in about 5.67 μm (see Figure 2C). Figures 2D and 2E show the energy-dispersive X-ray spectrum (EDS) and X-ray diffraction (XRD) patterns of three synthetic CRUD samples. XRD analysis shows that the main components are all nickel ferrite and iron oxide, and EDS analysis shows that the ratios of iron to nickel atomic number are 2.16, 2.21, and 2.18, respectively. The synthetic CRUD has good hydrophilicity, as the droplet completely penetrates into the porous medium within 0.12 s during a 5 μL sessile drop method contact angle measurement (Figure 2F).

The reason why the two-step method can be used to rapidly synthesize CRUD is that there are similarities with the formation mechanism of real CRUD,[21] as illustrated in Figure 3. At the beginning of the cycle, CRUD grows slowly at cladding surface defects by crystal growth, and the tiny corrosion product particles in coolant serve as the precursors of crystal growth. Subcooled boiling causes more dissolved corrosion products supersaturated and nickel ferrite crystal growth to be accelerated, making nickel ferrite the dominant crystal of CRUD. Boiling also increases the coolant flow to the cladding surface bringing more corrosion products into CRUD. Bubble departure through the porous medium

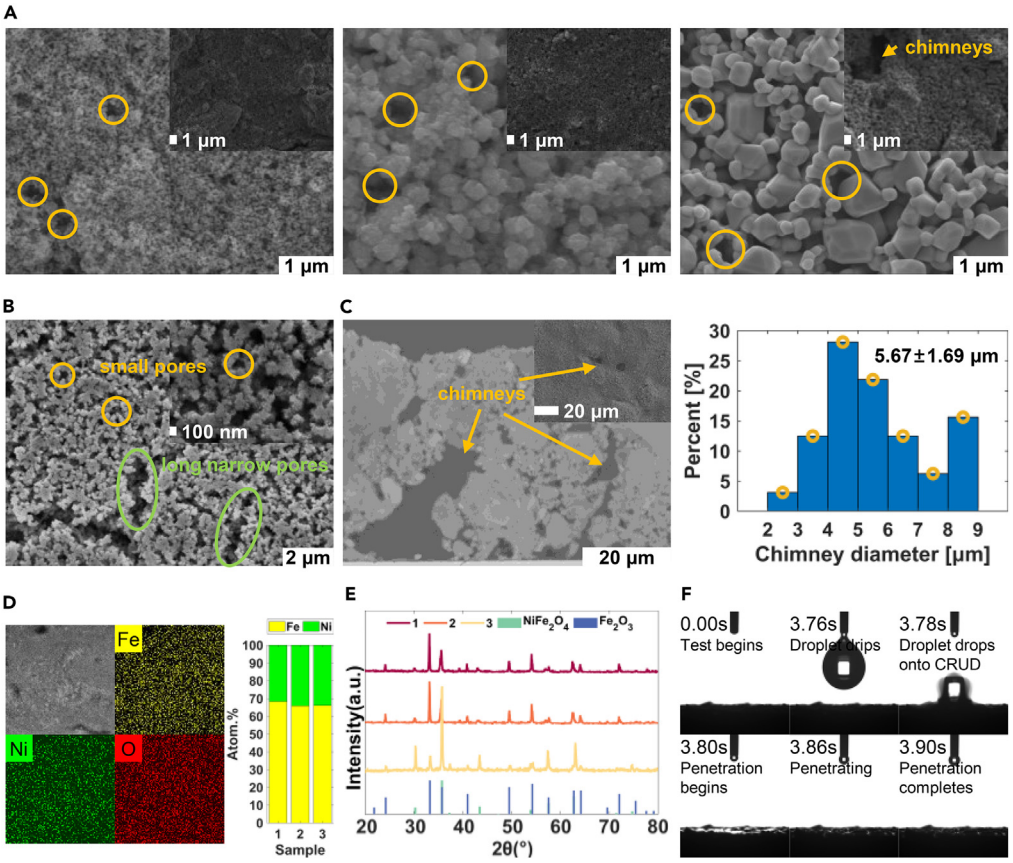

Figure 2. Characterization of the synthetic CRUD with different nanopowder sizes

(A) SEM images of three synthetic CRUD sample outer layer morphologies, including small pores and chimney structures.

(B) SEM images of three synthetic CRUD sample outer layer morphologies, including small pores and long narrow pores.

(C) SEM images of CRUD sample chimney top-down view and cross-sectional view, and chimney diameter distribution.

(D) Elemental map of three synthetic CRUD sample cross sections in (A).

(E) XRD patterns of the synthetic CRUD samples in (A).

(F) Water permeability of synthetic CRUD sample by contact angle measurement.

builds shallow boiling chimneys. Then after CRUD reaches a certain thickness, water chemistry changes as boron acid and lithium hydroxide are trapped in the thicker CRUD, making some nickel ferrite crystals dissolve and diffuse outward. A small amount of Fe_2O_3, NiO, or other substances precipitate in the CRUD outer half, leading to an obvious layering phenomenon. Meanwhile, more bubble escapes expand the original chimney. The whole process lasts for several months and is affected by various parameters in the reactor, forming CRUD depositions with different morphologies and different components.

Relatively speaking, the two-step rapid synthesis method greatly accelerates the crystal growth process, but the formation of the porous structure is still the result of gas generation and escape. In the first step, larger crystals are formed quickly, which deposit on the surface of the zirconium substrate after solvent evaporation and polymer decomposition. In the second step of the sintering process, the plasticizer and the pore-forming agent decompose into H_2O and CO_2 and leave the porous layer, forming a pore in the original position, and some gases escape after gathering forming chimneys. To some extent, since the mechanism of porous structure formation by the two-step synthesis method is similar to that of real CRUD growth, CRUD can be approximately simulated by this method theoretically and experimentally. Different CRUD morphologies and components can be synthesized by adjusting the experiment parameters, such as changing the polymer polymerization degree to control the inner layer's crystal sizes, changing the sintering temperature and nanopowder size to control the outer layer's crystal sizes and porosity, and changing the proportion of iron and nickel in the sol-gel and the nanopowder of the paste to control the composition.

Fractalline analysis

Measured fractal dimensions from the synthetic CRUD samples varied between experiment conditions, with the r^2 from log-log box-counting distribution all higher than 0.99. The close correlations also prove that the synthetic CRUD samples have strongly fractal characteristics. The relationship between the CRUD porosity and fractal dimension is shown in Figure 4C, combining two-step quick synthetic, IHTFP-grown[3] and

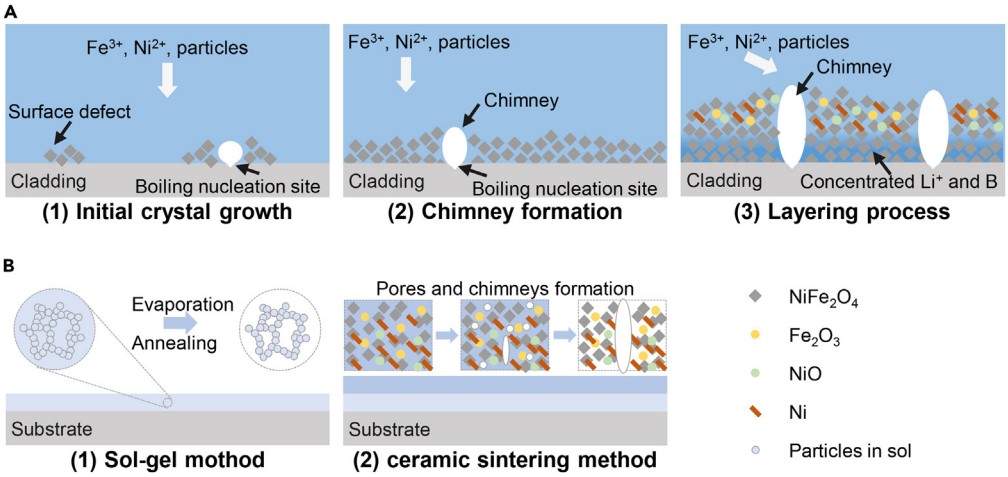

Figure 3. The mechanism feasibility of the synthesis method

(A) CRUD deposit growth mechanism, experiencing crystal precipitation and growth, solid skeleton and chimney formation, and layering process after reaching a certain thickness.

(B) CRUD synthesis mechanism, greatly reducing the time required for crystal precipitation and growth.

WALT-grown[2] CRUD samples. IHTFP loop[3] and WALT loop[2] simulated the reactor's typical thermal and hydrochemical conditions to grow CRUD, which were considered to be representative of the real CRUD samples. WALT loop, the non-nuclear experimental loop closest to the PWR conditions, is of great significance to understand the influence of reactor operating environment on CRUD deposition morphology and the feedback effect of CRUD porous morphology on heat transfer of fuel rods, which is also widely used to verify the accuracy of heat transfer simulation in CRUD. The data were in good agreement with the same logarithmic curve with the r^2 value higher than 0.99, indicating that these simulated CRUD samples have strong similarities. In general, the porosity of CRUD ranges from 40% to 70%.[1] The samples synthesized by the two-step rapid method can still fit this curve well at higher porosity, which also provided a larger range of porosity parameters for subsequent subcooled boiling and boron hideout experiments and theoretical predictions. Consistent with the pore structure parameter range of real CRUD, the best application range of fractal law is that the pore size is 0.1–1 μm and the porosity is between 40% and 70%. For comparison and verification, the CRUD specimens from Seabrook Cycle 5, Callaway Cycle 9, Vogtle 1, and VC Summer Cycle 12 reported by EPRI[21] were analyzed, as illustrated in Figure 4D. The real CRUD specimens from different reactors can also satisfy the fitted logarithmic curve well, with their maximum relative error less than 3%, which once again shows that the CRUD rapidly prepared by the two-step method can be used as a representative of the real CRUD to perform experiment. Although CRUD has extremely complex tortuous structures, it suggests that like other boiling fouling, CRUD are fractalline structures. Even though it is still difficult to define the self-similarity of CRUD, their complex pore structures can be considered to follow a self-similar law. Meanwhile, despite the different reactor operation conditions and CRUD structures, the similarity of the relationship between porosity and fractal dimension also provides a new perspective to analyze CRUD's depositions and their feedback impact on fuel performance and reactor operation. By associating fractal dimension with thermal conductivity, permeability, diffusion coefficient, and other parameters, it can help to find a consistent method to deal with the complex structures of CRUD in different reactors, so as to understand the safety concerns caused by CRUD more deeply and accurately.

Wick boiling and boron hideout performance

For all simulation cases, the CRUD internal temperature reaches the maximum at the junction of the cladding and the symmetry plane, while the maximum concentrations of aqueous boron and lithium solutes are at the junction of the chimney and the cladding. When the coolant enters the CRUD from the mainstream, the capillary fluid velocity is at its largest and almost flows along the axial direction. With the deepening, the velocity in this direction continues to decrease to 0, and the radial velocity at the chimney surface is increasing to its maximum. The pH value increases as it approaches the cladding because lithium ion concentrating controls the pH. Like in Figure 5B, on average, CRUD temperature at cladding surface reaches 626.331 K, which makes temperature difference between external and internal surfaces 9.243 K, and CRUD boric acid concentration at cladding surface reaches 0.782 mol/L, which is concentrated by 11.274 times compared with bulk coolant concentration. The difference is that there is no lithium tetraborate precipitation under some conditions (Figure 5B), which also shows the harsh conditions required for lithium tetraborate precipitation.

Figures 5C–5E shows the impacts of CRUD porosity, heat flux, and boron concentration in bulk coolant on boiling duty (evaporation steam flow) and boron species mass (both aqueous and solid) in the CRUD per unit surface area of the fuel rod, which are used to quantify wick boiling and boron hideout. With the increase of porosity, more water takes away heat and the boiling duty increases slightly. Meanwhile, the coolant has a smaller thermal conductivity than the metal oxide skeleton, meaning high-porosity CRUD has a smaller overall thermal conductivity, leading to a larger temperature difference between the inner and outer surfaces. The diffusion coefficient of boric acid modified by

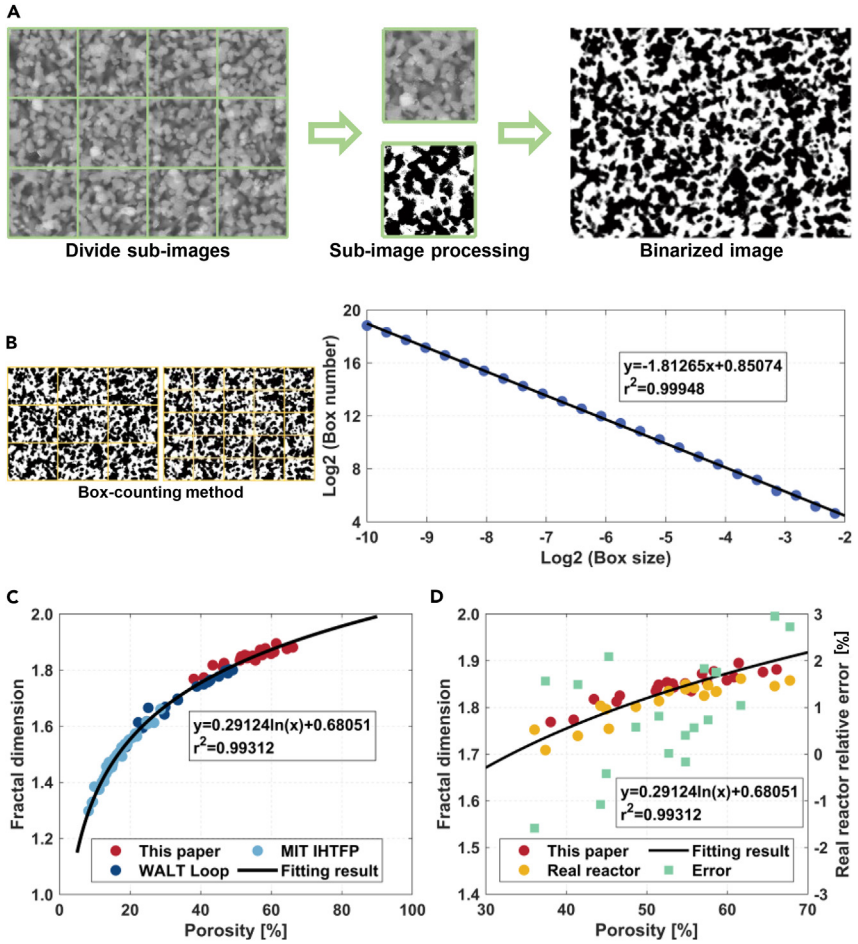

Figure 4. The process and comparison of the relationship between fractal dimension and porosity of CRUD

(A) Binarized image processing.

(B) Box-counting method used to obtain the CRUD fractal dimensions.

(C) Relationships between CRUD porosity and fractal dimension.

(D) Relationship between porosity and fractal dimension of real CRUD samples.

fractal theory increases with the increase of porosity, thus a larger diffusion coefficient needs only a smaller diffusion gradient to establish a balance between convection and diffusion. Therefore, the higher the porosity, the lower the boric acid concentration, and the lithium concentration also follows this trend, so does the boron species mass. When the porosity is less than 55%, lithium tetraborate begins to precipitate. Generally speaking, the higher the internal temperature of CRUD, the easier it is to cause zirconium cladding corrosion, leading to CILC. Meanwhile, higher boron concentration will cause larger depression in local neutron distribution, resulting in more serious CIPS.[13] Through the aforementioned analysis, it can be speculated that CRUD with high porosity is more likely to cause CILC, while CRUD with low porosity is more likely to cause severe CIPS. With the increase of heat flux, the proportion of heat taken away by evaporation at the chimney surfaces increases, and the boiling duty increases approximately linearly accordingly, which is similar to the analysis results of WALT loop experiment.[2] The strengthening of evaporation also increased the accumulation of boron, and lithium tetraborate was precipitated at 1.25 MW/m^2. Therefore, reactors with high heat flux under high power operation are more vulnerable to CILC and CIPS. The high concentration of boric acid in the bulk coolant can increase the saturation temperature. Under the same heat flux and CRUD morphology, the coolant with high boric acid concentration is more difficult to become saturated. The high boron concentration also naturally means more boron hideout, which also explains to some extent that Callaway Cycle 10 experienced CIPS at the beginning of the cycle[1] because of its high coolant boron concentration.

Conclusion

A two-step technical route combining sol-gel method with cermet sintering method was presented to rapidly reproduce PWR fouling deposit covering fouling deposit's morphologies and micro-structures. The comparison between the principle of the synthesis method and the formation mechanism of CRUD was carried out. A fractal study on fouling deposit's morphologies and micro-structures was conducted. In

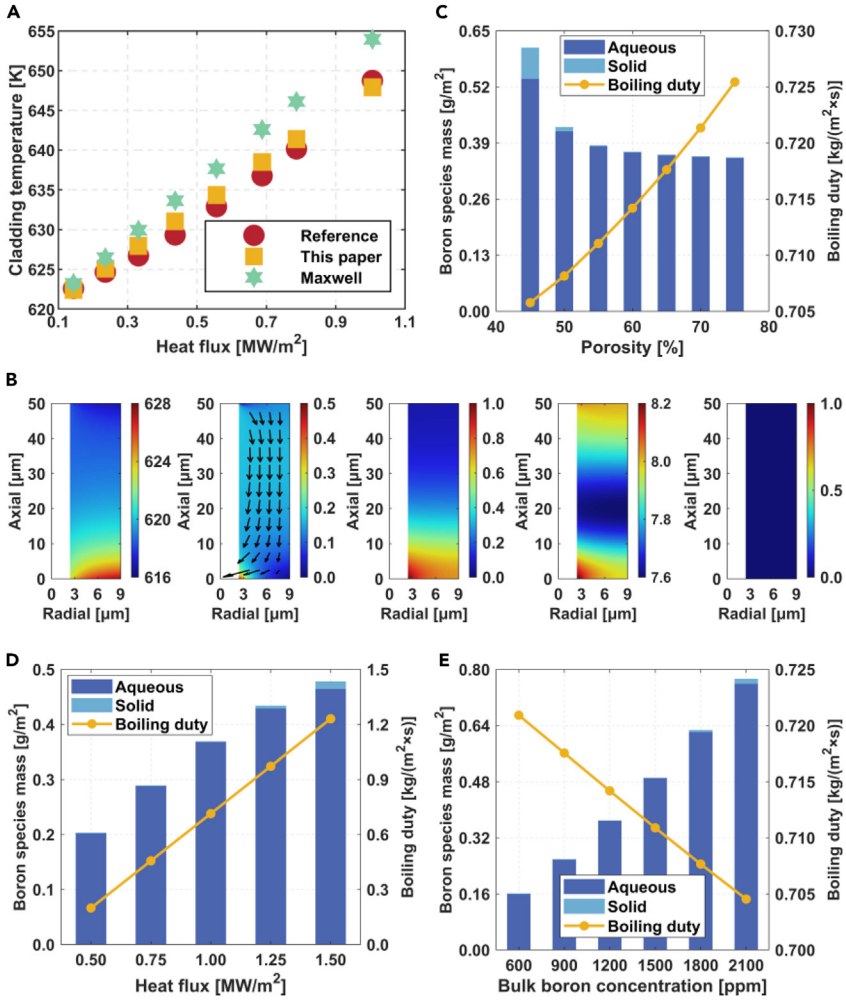

Figure 5. Verification and analysis of wick boiling and boron hideout simulation

Simulation results with common parameters: porosity, 60%; thickness, 50 μm; heat flux, 1.0 MW/m^2; bulk coolant boron concentration, 1200 ppm; bulk coolant lithium hydroxide concentration, 2.2 ppm; bulk coolant temperature, 608.15 K.

(A) The comparison between the temperatures (WALT Loop Rod 88) calculated via thermal conductivity corrected by fractal dimension in this paper and thermal conductivity obtained by Maxwell's formula.

(B) Variable distributions of 60% porosity CRUD: temperature (K), capillary fluid velocity (cm/s), boric acid concentration (mol/L), pH, and lithium tetraborate mass per unit area (g/m^2).

(C) CRUD porosity vs. boron species mass and boiling duty.

(D) Heat flux vs. boron species mass and boiling duty.

(E) Boron concentration in bulk coolant vs. boron species mass and boiling duty.

addition, a wick boiling and boron hideout simulation approach was established based on fractal dimension, which yielded important insights into the localized corrosion and power shift caused by the fouling deposit. The key conclusions drawn from this study include the following.

(1) A wide range of CRUD morphology parameters can be achieved by adjusting the synthesis parameters such as sintering temperature and iron-nickel ratio. The two-step method greatly saves time in crystal growth and deposition, while the principle of porous and chimney formation is similar, which proves the feasibility of the two-step method.

(2) Both fouling deposit synthetized by two-step method and fouling deposit from reactors are of self-similarity. Fouling deposit with different morphologies and structures are unified in the correspondence between porosity and fractal dimension.

(3) Compared to directly defining the physical properties of porous fouling layer, the introduction of fractal dimension can significantly reduce the wick boiling and boron hideout simulation error, showing reasonable agreement with the experimental results.

The results from this study provide a precise approach for quantitative evaluation of localized corrosion and power shift.

Limitations of the study

CRUD samples synthesized by the two-step method cannot achieve a fine density distribution along the radial direction of the fuel rod, that is, the inhomogeneity of the composition. At present, there is still a lack of density distribution analysis of real CRUD samples or synthetic CRUD samples via simulating thermal hydraulic conditions, which is mainly limited by measurement difficulty of CRUD micron scale. This makes the synthesis method lack reference in density distribution. One possible avenue for future research is to carry out *in situ* tests during the deposition process to obtain the fine density distribution of CRUD depositions and further improve the two-step synthesis method.

STAR★METHODS

Detailed methods are provided in the online version of this paper and include the following:

- KEY RESOURCES TABLE
- RESOURCE AVAILABILITY
  - Lead contact
  - Materials availability
  - Data and code availability
- METHOD DETAILS
  - Two-step synthetic method
  - Fractal dimension acquisition
  - Wick boiling and boron hideout theoretical simulation

SUPPLEMENTAL INFORMATION

Supplemental information can be found online at https://doi.org/10.1016/j.isci.2024.108789.

ACKNOWLEDGMENTS

This research has been supported by the National Natural Science Foundation of China (No. U20B2011 and 52176082), "Shu Guang" Project supported by Shanghai Municipal Education Commission and Shanghai Education Development Foundation (21SG13), and LingChuang Research Project of China National Nuclear Corporation.

AUTHOR CONTRIBUTIONS

Y.L.: methodology, experiment, data analysis, simulation, and writing – original draft. X.L.: conceptualization, investigation, methodology, writing – review and editing, funding acquisition, and supervision. H.H.: conceptualization, methodology, data analysis, simulation, writing – review and editing, and funding acquisition. T.Z.: investigation, data analysis, and simulation. X.C.: investigation, data analysis, and simulation.

DECLARATION OF INTERESTS

The authors declare no competing interests.

Received: August 15, 2023
Revised: November 8, 2023
Accepted: January 2, 2024
Published: January 4, 2024

REFERENCES

1. EPRI (2004). PWR Axial Offset Anomaly (AOA) Guidelines, Revision 1 (The Electric Power Research Institute).
2. EPRI (2010). Simulated Fuel CRUD Thermal Conductivity Measurements under Pressurized Water Reactor Conditions (The Electric Power Research Institute).
3. Dumnernchanvanit, I. (2017). Characterization and Mitigation of CRUD at Pressurized Water Reactor Conditions.
4. Macbeth, R.V. (1971). Boiling on Surfaces Overlayed with a Porous Deposit: Heat Transfer Rates Obtainable by Capillary Action (Atomic Energy Establishment).
5. Macbeth, R.V., Trenberth, R., and Wood, R.W. (1971). An Investigation into the Effect of "CRUD" Deposits on Surface Temperature, Dry-Out and Pressure Drop, with Forced Convection Boiling of Water at 69 Bar in an Annular Test Section (Atomic Energy Establishment).
6. McGrady, J., Duff, J., Stevens, N., Cioncolini, A., Curioni, M., Banks, A., and Scenini, F. (2017). Development of a microfluidic setup to study the corrosion product deposition in accelerated flow regions. npj Mater. Degrad. *1*, 21–29.
7. Turinsky, P.J., and Kothe, D.B. (2016). Modeling and simulation challenges pursued by the Consortium for Advanced Simulation of Light Water Reactors (CASL). J. Comput. Phys. *313*, 367–376.
8. Abdel-Khalik, S. (2005). Experimental Investigation of the Root Cause Mechanism and Effectiveness of Mitigating Actions for Axial Offset Anomaly in Pressurized Water Reactors (Georgia Institute of Technology).
9. Coyle, C.P. (2016). Synthesis of CRUD and its Effects on Pool and Subcooled Flow Boiling.
10. Sung, Y., Adams, B.M., and Secker, J.R. (2011). CASL L1 Milestone Report: CASL.P4.01, Sensitivity and Uncertainty Analysis for CIPS with VIPRE-W and BOA ((Sandia National Laboratories)).
11. EPRI (2017). Boron-Induced Offset Anomaly (BOA), Version 4.0 (The Electric Power Research Institute).
12. Mousseau, V.A., and Dinh, N. (2016). CASL Verification and Validation Plan (Sandia National Lab)).

13. EPRI (2004). Modeling PWR Fuel Corrosion Product Deposition and Growth Processes (The Electric Power Research Institute).
14. Zou, L., Zhang, H., Gehin, J., and Kochunas, B. (2012). A Coupled TH/Neutronics/CRUD Framework in Prediction of CIPS Phenomenon (Idaho National Lab).
15. Stanley, H.E., and Meakin, P. (1988). Multifractal phenomena in physics and chemistry. Nature *335*, 405–409.
16. Liu, X., Ma, J., Xu, S., and Wang, B. (2017). On the generation of coastline-following grids for ocean models—trade-off between orthogonality and alignment to coastlines. Ocean Dynam. *67*, 1095–1104.
17. Tang, H.P., Wang, J.Z., Zhu, J.L., Ao, Q.B., Wang, J.Y., Yang, B.J., and Li, Y.N. (2012). Fractal dimension of pore-structure of porous metal materials made by stainless steel powder. Powder Technol. *217*, 383–387.
18. Helalizadeh, A., Müller-Steinhagen, H., and Jamialahmadi, M. (2000). Mixed salt crystallisation fouling. Chem. Eng. Process: Process Intensif. *39*, 29–43.
19. Meng, F., Zhang, H., Li, Y., Zhang, X., Yang, F., and Xiao, J. (2005). Cake layer morphology in microfiltration of activated sludge wastewater based on fractal analysis. Separation and Purification Technology *44*, 250–257.
20. Yang, Q., Liu, Y., Gu, A., Ding, J., and Shen, Z. (2002). Investigation of induction period and morphology of CaCO3 fouling on heated surface. Chem. Eng. Sci. *57*, 921–931.
21. EPRI (2004). Evaluation of Fuel Clad Corrosion Product Deposits and Circulating Corrosion Products in Pressurized Water Reactors (The Electric Power Research Institute).
22. Sen, R., Jain, P., Patidar, R., Srivastava, S., Rana, R.S., and Gupta, N. (2015). Synthesis and characterization of nickel ferrite (NiFe2O4) nanoparticles prepared by sol-gel method. Mater. Today: Proc. *2*, 3750–3757.
23. Kim, Y.-H., Heo, J.-S., Kim, T.-H., Park, S., Yoon, M.-H., Kim, J., Oh, M.S., Yi, G.-R., Noh, Y.-Y., and Park, S.K. (2012). Flexible metal-oxide devices made by room-temperature photochemical activation of sol–gel films. Nature *489*, 128–132.
24. Rakmak, N., Wiyaratn, W., Bunyakan, C., and Chungsiriporn, J. (2010). Synthesis of Fe/MgO nano-crystal catalysts by sol–gel method for hydrogen sulfide removal. Chem. Eng. J. *162*, 84–90.
25. Zhang, D., Jonhson, W., Herng, T.S., Ang, Y.Q., Yang, L., Tan, S.C., Peng, E., He, H., and Ding, J. (2020). A 3D-printing method of fabrication for metals, ceramics, and multi-materials using a universal self-curable technique for robocasting. Mater. Horiz. *7*, 1083–1090.
26. Chen, I.-W., and Wang, X.-H. (2000). Sintering dense nanocrystalline ceramics without final-stage grain growth. Nature *404*, 168–171.
27. Zhu, J., Wu, P., Chao, Y., Yu, J., Zhu, W., Liu, Z., and Xu, C. (2022). Recent advances in 3D printing for catalytic applications. Chem. Eng. J. *433*, 134341.
28. Wu, M., Wang, W., Shi, D., Song, Z., Li, M., and Luo, Y. (2021). Improved box-counting methods to directly estimate the fractal dimension of a rough surface. Measurement *177*, 109303.
29. Wang, R., Singh, A.K., Kolan, S.R., and Tsotsas, E. (2022). Fractal analysis of aggregates: Correlation between the 2D and 3D box-counting fractal dimension and power law fractal dimension. Chaos, Solit. Fractals *160*, 112246.
30. Liang, H., Tsuei, M., Abbott, N., and You, F. (2022). AI framework with computational box counting and Integer programming removes quantization error in fractal dimension analysis of optical images. Chem. Eng. J. *446*, 137058.
31. Xu, P., and Yu, B. (2008). Developing a new form of permeability and Kozeny–Carman constant for homogeneous porous media by means of fractal geometry. Adv. Water Resour. *31*, 74–81.
32. Gierszewski, P., Mikic, B., and Todreas, N. (1980). Property Correlations for Lithium, Sodium, Helium, Flibe and Water in Fusion Reactor Applications (Massachusetts Institute of Technology).
33. Mesmer, R.E., Baes, C.F., and Sweeton, F.H. (1972). Acidity measurements at elevated temperatures. Inorg. Chem. *11*, 537–543.
34. Yu, B. (2008). Analysis of flow in fractal porous media. Appl. Mech. Rev. *61*.
35. Zhang, P., and Jia, H.W. (2016). Evolution of flow patterns and the associated heat and mass transfer characteristics during flow boiling in mini-/micro-channels. Chem. Eng. J. *306*, 978–991.
36. Reburn, W.T., and Gale, W.A. (1955). The system lithium oxide–boric oxide–water. J. Phys. Chem. *59*, 19–24.
37. Senyshyn, A., Boysen, H., Niewa, R., Banys, J., Kinka, M., Burak, Y., Adamiv, V., Izumi, F., Chumak, I., and Fuess, H. (2012). High-temperature properties of lithium tetraborate Li2B4O7. J. Phys. D Appl. Phys. *45*, 175305.
38. Teruel, F.E., and Rizwan-uddin. (2009). Characterization of a porous medium employing numerical tools: Permeability and pressure-drop from Darcy to turbulence. Int. J. Heat Mass Tran. *52*, 5878–5888.
39. Mandelbrot, B.B., Passoja, D.E., and Paullay, A.J. (1984). Fractal character of fracture surfaces of metals. Nature *308*, 721–722.
40. Shen, Y., Xu, P., Qiu, S., Rao, B., and Yu, B. (2020). A generalized thermal conductivity model for unsaturated porous media with fractal geometry. Int. J. Heat Mass Tran. *152*, 119540.

STAR★METHODS

KEY RESOURCES TABLE

REAGENT or RESOURCE	SOURCE	IDENTIFIER
Chemicals, peptides, and recombinant proteins		
Ammonium hydroxide	Aladdin	A112083-2.5L
Diethylene glycol	Yuanye	S24141-500ml
Ferric oxide nanopowders	Innochem	A24854
Ferroferric oxide nanopowders	Aladdin	I400322-1kg
Iron(III) nitrate nonahydrate	Meryer	M84859-500G
Nickel(II) acetate tetrahydrate	Meryer	M21021-500G
Nickel ferrite nanopowders	Picasso-e	BJS4902762
Nickel(II) oxide nanopowders	Innochem	A51906
Polyethylene glycol	Meryer	M86851-250G
Software and algorithms		
MATLAB 2022a	MathWorks	https://www.mathworks.com/
Python 3.7	Python Software Foundation	https://www.python.org/

RESOURCE AVAILABILITY

Lead contact

Further information regarding this manuscript and requests should be directed to the lead contact Xiaojing Liu (xiaojingliu@sjtu.edu.cn).

Materials availability

This study did not generate any new materials.

Data and code availability

All data reported in this paper will be shared by the lead contact upon request.

This paper does not report original code. All custom Python and MATLAB scripts will be available upon request.

Any additional information required to reanalyze the data reported in this paper is available from the lead contact upon request.

METHOD DETAILS

Two-step synthetic method

The key steps of the entire preparation procedure schematic diagram are shown in Note S1. CRUD samples with a double-layer structure were synthesized by a two-step method combining sol-gel method[22–24] and ceramic sintering method.[25–27] The inner layer was prepared via sol-gel method using nickel(II) acetate tetrahydrate ($Ni(CH_3COO)_2{\cdot}4H_2O$) and iron(III) nitrate nonahydrate ($Fe(NO_3)_3{\cdot}9H_2O$) taken in 1:2 stoichiometric molar ratio, respectively. The starting materials were dissolved in distilled water to form a 0.1 M solution. To make the starting materials fully ionized to obtain a homogeneous solution, the solution was magnetically stirred at 80°C for 2 hours. Some drops of polyethylene glycol (PEG) were added drop by drop as a capping agent. Subsequently, ammonium hydroxide was added drop by drop to the prepared solution. The above solution was magnetically stirred at 80°C for 6 hours to obtain a reddish brown sol. PEG chain absorbed and surrounded the nuclei caused by the nucleation of crystals to prevent their growth and control their size and shape. The clean and smooth substrate zircaloy-4 alloy was immersed in the prepared sol at a constant speed. After soaking for a while, the substrate was slowly and uniformly pulled up with a layer of sol-wet film on its surface. The substrate with the fabricated film was dried at 120°C for 10 minutes and then taken out and naturally cooled at room temperature for 10 minutes. The above steps were repeated some times till the ideal thickness, as the film thickness formed by once pulling was about 100-150 nm. After the last pull-up, the synthesized film was annealed at 500°C for 3 hours.

An iron-nickel paste consisted of ceramic/metal powders in a network of plasticizers, and macromolecular organic polymers. The paste was prepared by homogenizing different powders with plasticizer and macromolecular organic polymers using a simple mortar and pestle. The powder used can be a single powder or several powders mixed depending on the iron-nickel ratio and composition to be obtained. In particular, to minimize evaporation at room temperature, diethylene glycol (DEG) with low molecular weight and relatively low vapor pressure was selected as the plasticizer material. Meanwhile, DEG, whose absence may cause cracks in the sintered structure, can help disperse the

nanoparticles effectively. Macromolecular organic polymers were commonly used as pore-forming agents, which occupied a certain volume in the paste, decomposed and generated gas (usually CO_2 and H_2O) forming pores after calcination. In this study, PEG was chosen as the pore-forming agent material. The paste was coated on the surface of the prepared inner layer. Referencing TGA measurement shown in Figure S2A, the evaporation of the plasticizer and the debinding process were conducted at about 164.4°C and 328.3°C, respectively. The sintering process was conducted at 800°C in a high-temperature tube furnace considering the pore sizes and firmness (Notes S2 and S3). The ramping rate was set at 0.5°C/min for all heat treatment processes. To minimize cracking, a controlled cooling rate of 1°C/min to room temperature was employed.

Fractal dimension acquisition

Cross-section view and top-down view of CRUD SEM images were binarized to ensure the accuracy of the results. Generally, in order to avoid local dark areas being misjudged as pores within the CRUD, adaptive image contrast thresholding was applied to correct localized regions with different contrasts within the original images via Otsu's method. Finally, morphological image processing was used to remove the single-pixel artifacts caused by digital noise or small changes in contrast to avoid misidentifying a single pixel as a small pore. Previous research showed that the relative error of the fractal dimension obtained after the above steps was less than 2%,[28] which ensures the accuracy of the final results.

The processed binary images were analyzed via the box-counting method,[28–30] which measures the fractal dimension by calculating the number of boxes containing the corresponding pixels of the pores. By changing the size of the box, a series of corresponding box numbers containing pores were obtained. A linear best-fitting line was applied to the logarithmic data to generate a power-law fitting. The negative value of the obtained slope was the fractal dimension of the analyzed image. The images of synthetic CRUD samples were serially analyzed via the box-counting method, and the curves of CRUD fractal dimension and porosity with CRUD thickness were obtained. Figures 4A and 4B show the binarization process and the box-counting data process with a practical example in this study.

Wick boiling and boron hideout theoretical simulation

At present, the fractal theory has been used in the analysis of various porous materials. The physical parameters obtained by fractal theory are more accurate than the direct definition, and the results are more accurate.[31] Therefore, the relationship between porosity and fractal dimension obtained above was used to define various physical parameters in wick boiling and boron hideout predictions.

Within the CRUD depositions, the heat transfer, capillary flow, pressure drop, solute diffusion, convection transport and chemical reactions are closely related. Driven by subcooled boiling, the pressure drop between the chimney surface of CRUD and the interface with the coolant causes the coolant to enter the capillary micro-channels. Since the pore size is small enough, it is generally assumed that bubbles do not generate within the solid skeleton, the coolant only evaporates into steam at the chimney surface, and finally escapes through the chimneys into the bulk coolant, which in return strengthens this process. Since most solutes do not evaporate like water, they will be continuously concentrated in this process, such as H_3BO_3, Li^+ and $B(OH)_4^-$, but from a chemical point of view, there is always a chemical equilibrium between these solutes.[13,32–35] The continuously concentrated solutes influence the coolant saturation temperature, which in turn changes the evaporation at chimney surfaces and capillary flow, and thus affects the heat transfer and chemical equilibrium within the CRUD depositions. When the concentrations of boric acid and lithium ion reach a certain value, the saturation index of their precipitation reaction becomes positive, and lithium tetraborate will be precipitated and trapped in the porous structure of CRUD.[36,37] To simulate the aforementioned multi-physics coupling phenomena, a chimney and its surrounding porous structure are selected for the purpose of wick boiling and boron hideout predictions. The heat transferred to CRUD through the cladding is finally transferred to the bulk coolant through the evaporation at the chimney surface and the convective heat transfer at the interface between CRUD and the coolant. The low-velocity capillary flow within the porous CRUD depositions follows Darcy's low.[38] According to mass and element conservation, the change in solute concentration in the coolant is caused by diffusion, convection and chemical reactions. Due to the rapidity of reaction, solute transport and reaction within the CRUD depositions maintain in the quasi-steady state. The detailed modeling process is shown in Note S5.

In the simulation, the definitions of fluid permeability,[31] characteristic length[39] and thermal conductivity,[40] etc. can be simpler and more accurate with the application of fractal dimension. For example, the overall thermal conductivity takes better contribution from series and parallel conductivities in porous materials,[40] rather than simply weighting the volume fractions of solid and liquid thermal conductivity via Maxwell's formula. It can be found from the calculation of WALT Loop Rod 88 case that the temperature obtained by using the thermal conductivity defined by fractal dimension is in better agreement with the reference temperature, while the temperature error solved by Maxwell's formula increases with heat flux (Figure 5A). Fluid permeability expressed by porosity and fractal dimension is proved to be closer to the microstructure in the porous media than that defined by porosity only.[31] The relationship between porosity and fractal dimension can help to avoid the dependence of fractal dimension on the assumed pore size in some previous studies,[12] leading to smaller errors in some porosity cases. Thus the fractal analysis of CRUD can help to obtain more accurate physical parameters, resulting in more accurate heat and mass transfer simulation results within the CRUD depositions.